MURDOCH RESEARCH REPOSITORY

http://researchrepository.murdoch.edu.au/25013/

Reductive atmospheric acid leaching of lateritic smectite/nontronite ores in H_2SO_4/Cu(II)/SO_2 solutions

G. Senanayake[a], G.K. Das[b*], A. de Lange[b], J. Li[b], D.J. Robinson[b]

a. Chemical & Metallurgical Engineering & Chemistry, School of Engineering and Information Technology, Murdoch University, 90, South Street, Murdoch, Perth, WA6150, Australia
b. CSIRO Mineral Resources Flagship, Australian Minerals Research Centre, PO Box 7229, Karawara, Perth, WA6152, Australia

Abstract

Despite the success of reductive atmospheric acid leaching (RAAL) of limonitic nickel laterite ores in recent studies limited attempt has been made to apply this method to smectite/nontronite ores of different mineralogy. A comparative study of four smectite/nontronite ores in this study showed that the use of 700 kg H_2SO_4/ton dry ore leaches only 74-86% Ni, 37-76% Co, 47-58% Fe and 24-66% Mn at 90°C from slurries of 20-35% (w/w) pulp density even after 10 h, depending upon the mineralogy. These values increased to 90-97% Ni, 94-97% Co, 92-98% Mn and 72-85% Fe in the presence of Cu(II)/SO_2. The first order dependence of initial fraction of iron, aluminium and nickel leached from a typical smectite ore in the first 0.5 h on the initial acid concentration provide evidence for the involvement of hydrogen ions in the surface reaction. Low activation energy of 10 kJ/mol based on the fraction of nickel leached in the first 0.5 h indicates a diffusion controlled reaction. This is supported by the applicability of a shrinking core kinetic model for metal dissolution over the first 2 h, with different apparent rate constants (k_{ap}) depending upon the iron oxide content, mineralogy and porosity. A log-log plot of k_{ap} for ores with high iron content as a function of acid concentration agrees reasonably well with the correlation already established for the leaching of nickel from limonitic laterite and manganese nodules. Thus, initial fast leaching can be related to the higher porosity and a rate controlling step which involves the diffusion of H^+ through a thickening solid layer. The slow leaching at latter stages is a result of low remnant acid, thickening solid layer and changes in mineral composition.

Key words: Lateritic smectite/nontronite ores, Reductive acid leaching, Copper(II)/Sulphur dioxide, Kinetic models, Proton diffusion

*Corresponding author: Goutam.Das@csiro.au

1. Introduction

Processing of lateritic nickel ore through high pressure acid leaching (HPAL) is an established technology proven for extracting nickel from various lateritic ore bodies (Papangelakis et al., 1996; Rubisov et al. 2000; Whittington and Muir, 2000; Whittington and Johnson, 2005; Johnson et al., 2005). However, the atmospheric acid leaching (AAL) of nickel and cobalt from low grade laterite ores has drawn more attention recently (Buyukakinci and Topkaya, 2009) due to several reasons: (i) the depletion of high grade ore reserves and difficulty in upgrading the nickel contained in the ore through conventional techniques, (ii) the non-viability of HPAL process for the treatment of low grade laterite ores due to the higher capital expenditure and problems associated with materials of construction (Arroyo and Neudorf, 2002), (iii) the possibility of the precipitation of an intermediate mixed hydroxide precipitate (MHP) from clarified AAL liquors as a marketable product for refineries (Harvey et al., 2011). A number of companies are pursuing the development of potential atmospheric processes and a number of patents are in place; the recent reviews by McDonald and Whittington (2008a, 2008b) include the studies related to AAL of lateritic nickel ores. Despite the versatility of AAL process, a large excess of acid is required to dissolve the nickel bearing minerals in order to achieve acceptable leaching kinetics and efficiencies. Thus, large concentration of dissolved iron and residual acid in pregnant leach liquors affect the downstream processing (Buyukakinci and Topkaya, 2009). In general, the nickel leaching efficiencies vary from 40% to 90% depending on the mineralogy and process conditions and thus the AAL route for nickel laterite has not yet proven to be an attractive option to operate independently.

Studies have been reported on SO_2 accelerated leaching of various natural and synthetic iron oxides such as goethite, hematite, magnetite and nickel/cobalt spiked

goethite at atmospheric pressure (Surana and Warren, 1969; Warren and Hay, 1974; Byerley et al., 1979; Kumar et al., 1993; Petrie, 1995; Senanayake et al., 2011). The leaching of Mn from manganese ores, nodules, wads, etc. in the presence of a reducing agent is reported to be very effective (Grimanelis et al., 1992, Abbruzzese, 1990, Kanungo and Das, 1988, Canterford, 1984). Due to the strong reducing nature of SO_2, the dissolution of high-valent Mn-minerals is much faster (Das et al., 2000). Thus, reductive leaching under atmospheric conditions in the presence of SO_2 has been adapted to achieve more than 90% nickel and cobalt extraction from limonitic and saprolitic ores (Das et al., 1997; Das and de Lange, 2011; Kittelty, 2008; Lee et al., 2005; Senanayake and Das, 2004; Senanayake et al., 2011). The reductive leaching may prove to be a potential process option for future treatment of various lateritic ore bodies.

Although the oxidation of SO_2 to H_2SO_4 during the reductive leaching process allows for lower additions of H_2SO_4, the high leaching efficiency of iron oxides or oxy-hydroxides producing iron(II) species under reducing conditions is a disadvantage. Unlike in HPAL process in which iron(III) is precipitated as hematite at high temperatures, iron(II) produced during reductive leaching remains in solution. The leached iron(II) needs to be oxidised and precipitated prior to the production of MHP. The presence of copper(II) has a beneficial catalytic effect during SO_2 leaching of magnetite and laterite ores. Copper(I) ions produced by the reaction between sulphur dioxide and copper(II) act as a reducing agent (Byerley et al.,1979; Das et al., 1997; Senanayake et al., 2011). However, as copper(II) produced by the oxidation of copper(I) by high-valent metal oxides or oxy-hydroxides is reduced back to copper(I) by SO_2, the Cu(II)/(I) redox couple acts as a redox mediator. Previous studies on reductive atmospheric acid leaching (RAAL) have been mainly focussed on goethite

based limonitic ore from different origins using SO_2 as a reductant (Das et al., 1997; Kanungo et al., 1988; Senanayake and Das, 2004; Kittelty, 2008; Senanayake et al., 2011). A recent study has extended the AAL leaching system to nontronite type laterite ore from Western Turkey (Buyukakinci and Topkaya, 2009) and copper catalysed RAAL system to a smectite ore from Western Australia (Das and Lange, 2011; Das et al., 2010).

As shown in Fig. 1, the clay minerals of the smectite group are made up of layers of the cations Al^{3+}, Si^{4+} and Mg^{2+} along with the anions O^{2-} and OH^-, where two Si-centred tetrahedral sheets and one Al-centred octahedral sheet are bound with common oxygen atoms. Isomorphous substitution is extensive in smectite, with the substitution of Al^{3+} and Fe^{3+} for Si^{4+} in the tetrahedral sheets and Mg^{2+}, Fe^{3+} and Fe^{2+} for Al^{3+} in the octahedral sheets (Valenzuela-Diaz and Souza-Santos, 2001; Newman and Brown, 1987). Although less frequent, Cr^{3+}, V^{3+} and Zn^{2+} ions also are found as dominant cations in the octahedral sheets (Newman and Brown, 1987), there may also be other substitution such as Co^{2+} and Mn^{2+} in the octahedral site (http://www.britannica.com/EBchecked/topic/120723/clay-mineral/80130/Mica-mineral-group). The oxidation state of iron in smectite may vary between Fe^{3+} and Fe^{2+}, either through natural or laboratory processes which changes the chemical and physical properties such as colour, surface charge, surface area and swelling properties in water. Pores of diameters ranging from 2.0-6.0 nm correspond to 80% or more of the surface area of smectite. The acid treatment of smectite leaches cations from octahedral and tetrahedral sheets as well as the impurity metals by cation exchange with hydrogen ions (http://pubs.acs.org/doi/pdf/10.1021/bk-1990-0415.ch017).

Nontronite is the iron(III) rich member of the smectite group of clay minerals with typical chemical composition of more than ~30% Fe_2O_3 and less than ~12% Al_2O_3 (ignited basis). Nontronite can have variable amounts of adsorbed water associated with the interlayer surfaces and the exchange cations (http://webmineral.com/data/Nontronite.shtml). Table 1 lists the typical oxide compositions of some of these minerals indicating the presence of SiO_2, Al_2O_3, MgO and Fe_2O_3 at various percentages where one or more of these oxides become predominant in each case.

The AAL system for nickel leaching from smectite ore was slow and less efficient due to the fact that the nickel was found mainly in the crystal structure of goethite (α-FeOOH), serpentine $((Mg,Al,Fe,Mn,Ni)_{2-3}(Si,Al,Fe)_2O_5(OH)_4)$, smectite $(Mg_{0.2}(Fe_{1.2}Mg_{0.5}Ni_{0.1}Al_{0.3})(Si_{3.8}Al_{0.2})O_{10})(OH)_2.2H_2O)$ and asbolane $(Co,Ni)_{1-y}(MnO_2)_{2-x}(OH)_{2-2y}+2xn(H_2O)$ minerals (Buyukakinci and Topkaya, 2009; Das and Lange, 2011). This highlights the need for reducing agents to unlock the valuable metals such as nickel and cobalt. Although the effect of particle size, temperature, acid dosage and solid loading on metal ion leaching from smectite ores with H_2SO_4, SO_2/H_2SO_4 or $Cu(II)/SO_2/H_2SO_4$ have been studied in the past (Buyukakinci and Topkaya, 2009; Das et al., 2010; Das and Lange, 2011), further studies on comparison of different ores and kinetic modelling are warranted. In the present study the leaching of three different smectite ores of Western Australian origin was studied in $Cu(II)/SO_2/H_2SO_4$ system at the best conditions obtained from the previous study of the smectite ore by Das and Lange, 2011 (p.d. 35%, temperature 90 °C, time 10 h, H_2SO_4 ~600-700 kg/t ore) to understand the leaching variability of different smectite ores with an aim to achieve more than 90% nickel and cobalt extractions. The leaching results from this study were also compared and contrasted

with some of the published information under the AAL and RAAL conditions using Cu(II)/SO$_2$ as a reductant (Buyukakinci and Topkaya, 2009; Das et al., 2010; Das and Lange, 2011) and an attempt was made to rationalise the leaching kinetics.

2. Experimental

2.1 Sample preparation

Three smectite lateritic nickel ores from different mining locations in Western Australia identified as A, B, and C were used in this investigation for the purpose of comparing and contrasting the results with D (Das and Lange, 2011) and E (Buyukakinci and Topkaya, 2009) reported in the literature. The ore samples were air dried at ambient temperature for 48 h to reduce the moisture content prior to sample preparation. Dried ore was jaw crushed, roll-milled and sieved to minus 106 μm. The oversize fraction was pulverised, homogenised with the undersize fraction and stored in an air-tight bag. A sub-sample was collected from each laterite ore for moisture determination and to perform the chemical and mineralogical analyses prior to the leach test work.

2.2. Leaching procedure

Leaching experiments were carried out in a 2 L capacity continuously stirred baffled glass reactor fitted with a flat flange/multi-socket lid, with the sockets being fitted with quick-fit glass adaptors and a condenser to prevent evaporation losses. The reactor was heated in an oil bath (UltraPeg 400) with provision to control the bath temperature to maintaining the reactor temperature within $\pm 1°C$. The reduction was carried out by employing SO$_2$ gas in the presence of H$_2$SO$_4$. The standard

experimental conditions used for leaching were: pulp density 35% (w/w), temperature 90°C, agitation 450-500 rpm and duration 10 h.

A required amount of de-ionised (DI) water and sulphuric acid were transferred to the reactor and placed in the oil bath. Once the test temperature was attained inside the reactor, a calculated amount of dry ore was added. The addition of SO_2 gas at a flow rate of ~0.4-0.45 L/min (with the unused gas passing through the reactor being scrubbed in NaOH solution for safety) commenced immediately after the addition of ore. Part leached slurry samples were collected at a regular interval of time and filtered immediately. The solids were washed thoroughly and dried at 70°C. Intermediate solids and solutions were analysed for Ni, Co, Fe, Mg and Mn by ICP-OES using standard procedure. Free acid of the liquor was determined by pH titration using the standard oxalate method. The leaching studies for 10 h duration were conducted mostly using DI water adding 700 kg H_2SO_4/ton of ore at 90°C temperature with 35% w/w pulp density in the absence or presence of SO_2 gas and ~1 g/L Cu(II) as $CuSO_4.5H_2O$ added to the acid solution. The effect of H_2SO_4, H_2SO_4/SO_2 and $H_2SO_4/Cu(II)/SO_2$ was compared with previously reported data for different laterite ores.

3. Results and Discussion

3.1 Chemical and mineralogical analyses

The chemical and mineralogical analyses of the ore samples are given in Tables 2 and 3. The ores are mineralogically similar (Table 3) having nontronite as the major phase along with the unaccounted phases which are amorphous to XRD. Other mineral phases include serpentine, goethite, hematite, maghemite, chlorite, kaolinite and quartz. The distribution of nickel in various mineral phases for different

Western Australian smectite ores were reported to be ~70-80% in smectite/nontronite and the rest was associated with goethite, chlorite and serpentine minerals (McDonald and Whittington, 2008a; Watling et al., 2011). It is expected that a similar nickel distribution may occur in the smectite samples used in this study. Figs. 2a-b illustrates the correlations of assays of metals in the feed material. The cobalt and manganese contents increase with the increase of nickel content (Fig. 2a) in these ores. Likewise, the chromium content increases with the increase in iron content but the silicon content shows the opposite behaviour (Fig. 2b). Table 4 shows that the chemical analysis of 10 h leach residues gave a lower nickel content when $Cu(II)/H_2SO_4/SO_2$ was used as the lixiviant in the RAAL system. This indicates that it is possible to achieve about 0.1% or less Ni in the RAAL leach residue of some ores depending upon the pulp density and acid dosage.

Previous studies showed that the smectite and goethite peaks in XRD scans of the ore E described in Tables 2 and 3 were absent in the XRD scans of the leach residue produced with AAL system (Buyukakinci and Topkaya, 2009). Fig. 3 compares the XRD traces of the ore C feed and the two leach residues obtained using H_2SO_4 and $H_2SO_4/Cu(II)/SO_2$ as lixiviants in the present study. The nontronite present in the ore C was found to be incompletely dissolved after 10 h of leaching in the presence of $Cu(II)/SO_2$ (Fig. 3). The XRD traces of the 10 h H_2SO_4 leach residue produced in the absence of $Cu(II)/SO_2$ show a reasonably higher nontronite peak. However, the peak intensity was significantly reduced in the residue in the presence of $Cu(II)/SO_2$. The difference of the nontronite peak height indicates that, $Cu(II)/SO_2$ has an important role in acid leaching to dissolve the nontronite phases by reducing

Fe(III) to Fe(II) leading to higher metal extractions. The leaching data of ore C is discussed in the section 3.3.2.

3.2 Leaching behaviour

3.2.1 Effect of leaching reagents

Previous studies on redox behaviour of Fe(III)/Fe(II) couple in smectite indicated the possibility of over 90% reduction of Fe(III) to Fe(II) where the rate of reduction increased with the amount of the reducing agent (Komadel et al., 1995). The co-existence of nickel, cobalt and manganese in the porous oxide/silicate structure (Figs.1-2) highlights the importance of comparing the leaching efficiencies (LE) of these metals as well as iron in H_2SO_4, SO_2, H_2SO_4/SO_2 and $H_2SO_4/Cu(II)/SO_2$ in order to examine the effect of acid and reducing agent. Table 5 shows a general comparison of LE of metals from ore D after 10 h using different lixiviants/conditions based on the data reported by Das and Lange (2011).

Sulphur dioxide dissolved in water is a weak acid ($SO_2 + H_2O = H^+ + HSO_3^-$) as indicated by the low equilibrium constant $K_a = 10^{-2}$ ($pK_a = 2$) at 25 °C. The increase in temperature causes a decrease in SO_2 solubility (mol/L) and an increase in pK_a (Senanayake et al., 2011). Thus, the lower LE of < 20% for Fe, Ni and Mg after 10 h was observed in test (ii) with SO_2 alone as the lixiviant. The increase in $LE_{(Fe)}$ from 10% to 47% and $LE_{(Ni)}$ from 16% to 75% when the lixiviant was changed from a weakly acidic solution of SO_2 (Test (ii)) to a strongly acidic solution of H_2SO_4 (Test (i)) indicates the enhanced oxide leaching in the presence of strong acid.

Fig. 4a shows the ascending order of $LE_{(Fe)}$ and $LE_{(Ni)}$ caused by different reagents: $SO_2 < SO_2/Cu(II) << H_2SO_4 < SO_2/H_2SO_4 < SO_2/Cu(II)/H_2SO_4$. This is an indication of the significant beneficial effect of the presence of H_2SO_4. The lixiviant order for $LE_{(Co)}$ and $LE_{(Mn)}$ is $H_2SO_4 < SO_2 < SO_2/Cu(II) < SO_2/H_2SO_4 \approx$

SO_2/Cu(II)/H_2SO_4 (Fig. 4b). The values of $LE_{(Co)}$ and $LE_{(Mn)}$ were approximately 60% or more with SO_2 alone (Test (ii) in Table 5). Thus, SO_2 facilitates the reductive leaching of hi-valent Co and Mn according to the reactions in Eqs. 1 and 2 (Liu et al., 2004; Lee et al., 2005; Das et al., 1997; Senanayake and Das, 2004; Senanayake et al., 2011). However, the presence of $FeSO_4$ produced by the reductive acid leaching of iron(III) oxides by SO_2/H_2SO_4 may facilitate the reductive leaching according to Eqs. 3-4 (Kyle, 1996; Rubisov and Papangelakis, 2000; Ferron and Henry, 2008; Senanayake et al., 2011).

$$(Mn,Co)O_2+SO_2+H_2SO_4=MnSO_4+CoSO_4+H_2O \qquad (1)$$

$$MnO_2+SO_2=MnSO_4 \qquad (2)$$

$$MnO_2+2FeSO_4+2H_2SO_4=MnSO_4+Fe_2(SO_4)_3+2H_2O \qquad (3)$$

$$2CoOOH+2FeSO_4+3H_2SO_4=2CoSO_4+Fe_2(SO_4)_3+4H_2O \qquad (4)$$

Likewise, even in the absence of H_2SO_4 the Cu(II)/SO_2 system facilitates the leaching of Mn and Co due to the reductive role of Cu(I) produced by the reaction between Cu(II) and SO_2 (Das et al., 1997; Das and Lange, 2011; Senanayake et al., 2011). The maximum values of $LE_{(Co)}$ and $LE_{(Mn)}$ from the smectite ore D vary in the range 95-97%, in comparison to almost 100% in the case of limonites (Senanayake and Das, 2004; Senanayake et al., 2011). Table 5 shows that the value of $LE_{(Fe)}$ in the weak acid SO_2 in Test (ii) is nearly doubled (from 10.3% to 22.4%) caused by Cu(II)/SO_2 in Test (iii). This appears to be due to the reductive role of Cu(I) on other metal oxides in the lattice which facilitate iron leaching. The $LE_{(Mg)}$ is also nearly doubled from Test (ii) to (iii) which is possibly due to the breakage of smectite matrix by reductive role of Cu(I) causing the dissolution of magnesium. In strongly acidic conditions $LE_{(Fe)}$ increased from 72.5% in Test (iv) to 83.6% in Test (v) indicating the effect of copper on the iron dissolution from the ore is not significant.

The acid dissolution mechanism of multi-oxide-silicate minerals is proposed by Oelkers (2001) which can be applied to explain the dissolution of smectite/nontronite minerals. The dissolution mechanism follows a sequential breaking of metal-oxygen bonds in the order of monovalent > divalent > trivalent > tetravalent, releasing various metals from the mineral surface into solution. Once the inter-layer monovalent cation (e.g. $\sim Na^+/K^+$) and/or divalent cation (e.g. $\sim Mg^{2+}/Ca^{2+}$) oxygen bonds in the exchange site of nontronite are broken initially in the dissolution process, then the ferric iron-oxygen bond sitting in the tetrahedral site of the nontronite structure would be exposed to SO_2/H_2SO_4 attack. From this point the dissolution mechanism of smectite/nontronite is expected to follow SO_2 assisted reductive dissolution similar to the reductive breakage of iron-oxygen bond during the dissolution of limonitic goethite minerals in acidic solution in the presence of SO_2 or $SO_2/Cu(II)$ (Das et al., 1997; Senanayake and Das, 2004). The enhanced leaching efficiency of metals from smectite/nontronite ores in the reductive leaching with $SO_2/Cu(II)/H_2SO_4$ system may follow this proposed mechanism, however, further work is warranted to support this theory.

3.3.2 Comparison of ores

Tables 6 and 7 list the acid dosage, initial and final concentrations of acid and the leaching efficiencies of metals from different laterite ores in experiments conducted in this work as well as in other studies. In all cases the nickel extraction increased with the initial acid dosage indicating the need for acid to enhance kinetics and leaching efficiency of nickel. Acid dosages equal to or higher than 600 kg/t are essential for the extraction of over 90% nickel from smectite ores. The residual acid is also higher at higher initial acid dosages (Table 6). The apparent acid consumption for the ores A, B and C at 700 kg H_2SO_4 per ton of ore in the $H_2SO_4/Cu(II)/SO_2$ system

were calculated to be approximately 543 kg/t ore, 588 kg/t ore and 552 kg/t ore when where $LE_{(Ni)}$ were found to be 96.9%, 95.1% and 94.4%, respectively.

Figs. 5a-d show the leaching curves for Ni, Fe, Co and Mn in H_2SO_4 alone and H_2SO_4/Cu(II)/SO_2 to show the leaching behaviour of different smectite ores in AAL and RAAL processes. In the absence of Cu(II)/SO_2 the relative leaching efficiencies in H_2SO_4 follow the general order Ni > Fe > Co > Mn for all four ores. This agrees well with the previous discussion given in section 3.1 on the dominant part of the nickel association with nontronite/smectite for ore A-D which is relatively easy to leach even without reductant (Watling et al., 2011; Gaudin et al., 2005a). Another common feature in the curves in Figs. 5a-d is that the metal leaching in H_2SO_4 alone is dramatically slowed down after 2 h. For example, $LE_{(Fe)}$ reached a plateau after 4 h and there is no significant change of $LE_{(Fe)}$ over the last 6 h. In all cases $LE_{(Fe)}$ remained less than 60% even after 10 h.

Although, the value of $LE_{(Fe)}$ continued to increase in H_2SO_4/Cu(II)/SO_2 it was less than $LE_{(Ni)}$. This behaviour is different from the leaching of iron and nickel from limonitic laterite ores, where the two are equally benefitted by the reducing agents. Due to the fact that nickel is associated with the goethite lattice of limonitic ores a plot of $LE_{(Ni)}$ as a function of $LE_{(Fe)}$ showed a linear relationship of slope close to unity (Senanayake and Das, 2004; Senanayake et al., 2011). Fig. 6 shows a similar plot of $LE_{(Ni)}$ as a function of $LE_{(Fe)}$ based on Figs. 5a-b for H_2SO_4 leaching in the absence or presence of Cu(II)/SO_2 for ores A-D. Although there is a general linear relationship of slope close to 1.2 most of the data points for nickel leaching are well above those for iron leaching. Despite the slow leaching kinetics, the lower values of $LE_{(Fe)}$ compared to $LE_{(Ni)}$ of smectite ores is an advantage in the downstream processing steps for the removal of iron from the leach liquors. The large chemical

variability in different Fe-rich smectite produced from laterite weathering profiles can be related to the substitution of the three major cations (Fe, Al, Mg) within adjacent octahedra in the structure depicted in Fig.1. The fact that nickel is located in the octahedral sheets of smectite in separated Fe, Al, Mg clusters (Gaudin et al., 2005a,b) warrants further analysis of results in Figs. 5a-d.

Fig. 7a-d show plots of $LE_{(Ni)}$ as a function of $LE_{(Fe)}$ for the leaching of ores A-D in H_2SO_4 or $H_2SO_4/Cu(II)/SO_2$ systems. In the case of reductive leaching with $H_2SO_4/Cu(II)/SO_2$ the slopes vary in the order C (0.51) < D (0.84) < B (0.95) < A (1.16). Ore B which has a slope closer to unity (0.95, Fig.7b) has the highest goethite content of 11.2% (Table 3). Thus, Fig. 8 plots the slopes of Figs. 7a-d as a function of the elemental assay of Fe (%) or the total mass percentage of iron oxide/oxyhydroxide minerals (%) in ores A, B, C and D reported in Tables 2 and 3. The lower slopes are associated with lower iron content in ores.

Likewise, Fig. 9 plots the slopes and intercepts of the linear relationships of Figs. 7a-d as well as $LE_{(Ni)}$ after 0.5 h of leaching in AAL and RAAL systems, as a function of the molar ratio of Fe/(Fe+Mg+Si) in ores. A low iron molar ratio in the laterite structure corresponds to lower slope but higher intercepts and higher values of $LE_{(Ni)}$ after 0.5 h. This indicates that the oxide/silicate structures with lower iron content (e.g. ore C) contains a larger fraction of nickel which can be subjected to faster leaching even in the absence of a reducing agent. The difference between $LE_{(Ni)}$ (RAAL) and $LE_{(Ni)}$ (AAL) in Fig. 9 shows that the reductive leaching improves the nickel leaching efficiency after 0.5 h by 10-15% depending upon the ore.

The different behaviour of ore C, presumably due to low iron content, is further examined in Fig.10 by plotting the values of $LE_{(Ni)}$, $LE_{(Mn)}$ and $LE_{(Co)}$ as a function of $LE_{(Fe)}$ under AAL and RAAL conditions to compare the leaching

behaviour of different metals from this ore. Under both non-reducing (AAL) and reducing (RAAL) conditions the data points for $LE_{(Ni)}$ as a function of $LE_{(Fe)}$ follow the same curve. Moreover, the fact that the leaching of both Fe and Ni is facilitated by the reducing agent confirms the necessity to break the iron/smectite lattice to leach nickel. In contrast the values of $LE_{(Mn)}$ and $LE_{(Co)}$ are lower than $LE_{(Fe)}$ under non-reducing conditions. However, under reducing conditions the values of $LE_{(Mn)}$ and $LE_{(Co)}$ are higher than $LE_{(Ni)}$ indicating the direct involvement of $Cu(II)/SO_2$ in the leaching of these metals. This situation is similar to that for ore-D shown in Fig 4b.

The published Eh-pH diagrams and other information for $Mn-Co-Fe-H_2O$ system show that divalent Fe(II) and Mn(II) produced by partial dissolution of Fe_3O_4 and Mn_3O_4 can be involved in reductive leaching of high-valent Co-Mn oxides (Zhang et al., 2002; Senanayake, 2011; Senanayake et al., 2011). A certain fraction of iron associated with the smectite structure and mineralogical formulae of silicates noted in Fig. 1 and Table 3 may be slow leaching, compared to the iron associated with oxide/oxy-hydroxide minerals. Some of these observations warrant further studies and analysis based on kinetic models as described in the next section.

3.3 Leaching kinetics

The increase in temperature from 85^oC to 90^oC and 95^oC has a beneficial effect on ore-D and increases the leaching efficiency of nickel from 85.6% to 88.6% and 90.8%, respectively, in $H_2SO_4/Cu(II)/SO_2$ (Das and Lange, 2011). Fig. 11 shows an Arrhenius plot of the initial rates Ln(dX/dt) for the leach results after 0.5 h at the three different temperatures (Das and Lange, 2011) as a function of $-1000/(8.314\ T)$, where X is the fraction of nickel leached after time t and T is the absolute

temperature. The slope of the linear relationship corresponds to activation energy of $E_a \approx 10$ kJ/mols which indicate a diffusion controlled reaction (Levenspiel, 1972).

The relative dependence of metal leaching on ore type and the diffusion controlled nature of reaction kinetics can be further examined on the basis of heterogeneous kinetic models. Previous studies have shown the applicability of a shrinking core kinetic model for the dissolution of Fe and Ni from limonitic nickel laterite ores, manganese nodules and Ni-Al$_2$O$_3$ spent catalysts (Gergeou and Papangelakis, 1998; Parhi et al., 2013; Senanayake and Das, 2004; Senanayake, 2011; Senanayake et al., 2011). For the dissolution of metals from particles in batch reactors represented by the general reaction A(aq) + bB(s) → products, where A is the active reagent of the lixiviant, a shrinking core model assumes that the diffusion of a reactive species or product through a porous solid layer of increasing thickness is the rate controlling step. The mathematical expression for this kinetic model is given by Eq. 5, where, b = stoichiometric factor, c_A = average concentration of A (mol cm^{-3}), ρ_M = concentration of the dissolving metal in the particle (mol cm^{-3}), r = particle radius (cm), D = diffusivity of the species through a product layer (cm^2 s^{-1}) and ε = particle porosity (Levenspiel, 1972; Gergeou and Papangelakis, 1998).

$$1 - 3(1-X)^{2/3} + 2(1-X) = \left(\frac{6bDc_A}{(1-\varepsilon)\rho_M r^2} \right)t = k_{ap}t \tag{5}$$

Fig. 12 shows the linear relationship between $1-3(1-X)^{2/3}+2(1-X)$ and time (t) for the leaching of Ni, Fe, Co and Mn from ore A. The apparent rate constant based on the slope of such linear relationships for the four types of ores are listed in Table 8. According to Eq. 5, the magnitude of k_{ap} depends on the terms such as ρ, c, r, D and ε. Previous studies have shown that particle size has no significant influence on leaching efficiencies of metals from smectite ores (Das and Lange, 2011; Buyukakinci and

Topkaya, 2009) which is consistent with the high porosity of laterite ores. For example, the porosity and surface area of a laterite ore has been reported as 0.708 and 64.82 $m^2 g^{-1}$, respectively. Smectite has pores with diameters ranging from 2.0-6.0 nm which correspond to 80% or more of the surface area (Valunzuela-Diaz and Souza-Santos, 2001). The surface area can vary in the range 40-800 $m^2 g^{-1}$ (http://www.britannica.com/EBchecked/topic/120723/clay-mineral/80136/Imogolite-and-allophane#toc80137). Moreover, Fig. 13 shows that k_{ap} is generally proportional to the initial leaching rates dX_M/dt of the metals (Ni, Fe, Co and Mn). Higher initial rates and k_{ap} values as a result of higher porosity lead to higher leaching efficiencies (Fig. 5).

Previous studies have shown that the initial rate (dX/dt) of leaching of iron from limonitic laterite in the presence of SO_2/H_2SO_4 obeys a first order dependence on the concentration of H^+ (Senanayake and Das, 2004). Likewise, Fig. 14a shows log-log plots of initial leaching rates of iron, aluminium, nickel, cobalt and manganese from ore D as a function of H^+ concentration based on the initial H_2SO_4 dosage reported in Table 9. The slopes of the linear relationships are close to unity in the case of iron, aluminium and nickel. However, the initial leaching rates of cobalt and manganese which are higher than aluminium, iron and nickel, are less dependent on H^+ concentration with a slope of 0.17. Moreover, it is of interest to note that the initial leaching rates of silicon, magnesium and chromium correspond to slopes closer to zero at low acid concentrations (Fig. 14b). Despite the large silica content in ore D, the leaching of silica remains very slow and low except at strong acid dosages, according to Table 9. These results indicate the involvement of H^+ in the surface reaction of the acid dissolution of iron, aluminium and nickel from ore D and the need for the diffusion of H^+ through the silicate/oxide matrix (Fig. 1).

The first order dependence of k_{ap} on c has been confirmed using a plot of $\log\{k_{ap}\}$ as a function of $\log\{c\}$ which showed a linear relationship of slope close to unity: $\log\{k_{ap}\} = 1.04 \log\{c\} - 8.17$ for the leaching of iron and nickel from manganese nodules and limonitic laterite ores during AAL or RAAL processes (Senanayake, 2011). The values of k_{ap} for nickel leaching from smectite ores A-D during AAL and RAAL processes (Table 8) are also included in the logarithmic plot in Fig. 15. The value of k_{ap} for ore-A which contains the highest iron content in Table 2 agree well with the linear relationship in Fig. 15. This supports the view that the diffusion of H^+ through a thickening porous product layer is the rate controlling step, as in the case of limonite and manganese nodules proposed previously (Senanayake and Das, 2004; Senanayake, 2011). The concentrations of acid used in the case of different smectite ores reported in Table 6 are also comparable. Thus, the slight deviations from the linearity observed in Fig. 12 at higher concentrations can be largely a result of the differences in porosity of the solid phases and/or the diffusion coefficient of H^+ in each case. It is likely that the initial leaching of iron and nickel in the form of oxides/oxy-hydroxides obey the shrinking core kinetics over the first 1-2 h as shown in Fig. 12. The leaching of metals from the smectite structure at later stages occurs at a much slower rate, as shown in Figs. 5a-d, due to low remnant acid and different porosity/mineralogy.

4. Conclusions

Atmospheric acid leaching of smectitic ores (clay based nontronite) was very effective in the presence of Cu(II)/SO$_2$, giving (i) more than 90% Ni and Co extraction and (ii) low Ni analysis in the residue. The different smectite ores gave 75-86% Ni and 51-59% Fe extractions when leached with 700 kg H$_2$SO$_4$/ton of dry ore without Cu(II)/SO$_2$, whereas for leaching in the presence of Cu(II)/SO$_2$ produced

more than 94% Ni and 80-85% Fe extractions. The residue analysis for nickel was 0.09-0.23% for leaching with $Cu(II)/SO_2$, and 0.27-0.68% without $Cu(II)/SO_2$. Most of the Co and Mn content was leached within half an hour of reaction in the presence of $Cu(II)/SO_2$ when cobalt was associated with manganese minerals. However, the effect of $Cu(II)/SO_2$ was not significant on magnesium extraction as most of it took place under normal acid leaching conditions without SO_2. Initial leaching of iron, nickel, cobalt and manganese from smectite ores obey shrinking core kinetics. The logarithmic correlation of apparent rate constants for nickel leaching and concentration of H^+ follow the same linear relationship as that reported for manganese nodules and limonitic laterite.

5. Acknowledgements

9. References

Abbruzzese, C., 1990. Percolation leaching of manganese ore by aqueous sulphur dioxide. Hydrometallurgy 25, 85-97.

Arroyo, C., and Neudorf, D., 2002. Atmospheric leach process for the recovery of nickel and cobalt from limonite and saprolyte ores. US patent 20020041840. April 2002.

Bayliss, P., 1975. Nomenclature of the trioctahedral chlorites. Canadian Mineralogist 13, 178-180.

Brigatti, M.F., Galli, E., Medici, L., Poppi, L., 1997. Crystal structure refinement of aluminium lizardite-2H $_2$. American Mineralogist 82, 931–935.

Büyükakinci, E. and Topkaya Y.A., 2009. Extraction of nickel from lateritic ores at atmospheric pressure with agitation leaching. Hydrometallurgy 97, 33-38.

Byerley, J.J., Rempel, G.L. and Garrido, G.F., 1979. Copper catalysed leaching of magnetite in aqueous sulphur dioxide. Hydrometallurgy 4, 317-336.

Canterford, J.H., 1984. Cobalt extractions and concentration from manganese wad by leaching and precipitation. Hydrometallurgy 12, 335-354.

Das, G.K., Anand, S., Das, R.P., Muir, D.M., Senanayake, G., Singh, P. and Hefter, G., 1997. Acid leaching of nickel laterites in the presence of sulphur dioxide at atmospheric pressure. In: Cooper, W.C. and Mihaylov, I. (Eds.), Proceedings of the Nickel-Cobalt 97 International symposium, Hydrometallurgy and Refining of Nickel and Cobalt – Vol. 1, Canadian Institute of Mining, Metallurgy and Petroleum, Montreal, pp. 471-488.

Das, G.K., Anand, S., Das, R.P., Muir, D.M. and Singh, P., 2000. Sulphur dioxide – A leachant for oxidic materials in aqueous and non-aqueous media. Min. Proc. Ext. Met. Rev. 20, 377-407.

Das, G.K., de Lange, J.A.B., 2011. Reductive atmospheric acid leaching of West Australian smectitic nickel laterite in the presence of sulphur dioxide and copper(II). Hydrometallurgy 105, 264–269.

Das, G.K., de Lange, A., Li, J., Robinson, D.J., 2010. Superior atmospheric leaching of various West Australian laterite in the presence of sulphur dioxide. ALTA, Melbourne, 2011, pp. 1-15.

Ferron, C.J., Henry, P., 2008. The use of ferrous sulphate to enhance the dissolution of cobalt minerals. In: Young, A.C., Taylor, P.R., Anderson, C.G., Chi, Y. (Eds.), Hydrometallurgy 2008 — 6th International Symposium, SME, Littleton, pp. 1088–1097.

Gaudin, A., Grauby, O., Noack, Y., Decarreau, A., Petit, S., 2005a. Accurate crystal chemistry of ferric smectites from the lateritic nickel ore of Murrin Murrin (Western Australia). I. XRD and multi-scale chemical approaches. Clay Minerals 39, 301-315.

Gaudin , A., Petit, S., Rose, J., Martin, F., Decarreau, A., Noack, Y. , Borschneck, D., 2005b. The accurate crystal chemistry of ferric smectites from the lateritic nickel ore of Murrin Murrin (Western Australia). II. Spectroscopic (IR and EXAFS) approaches. Clay Minerals 39, 453-467.

Georgiou, D., Papangelakis, V.G., 1998. Sulphuric acid pressure leaching of a limonitic laterite: chemistry and kinetics. Hydrometallurgy 49, 23–46.

Grimanelis, D., Neou-Syngouna, P., Vazarlis, H., 1992. Leaching of a rich Greek manganese ore by aqueous solutions of sulphur dioxide Hydrometallurgy 31, 139-146.

Harvey, R., Hannah, R., Vaughan, J., 2011. Selective precipitation of mixed nickel-cobalt hydroxides. Hydrometallurgy 105, 222-228.

http://pubs.acs.org/doi/pdf/10.1021/bk-1990-0415.ch017

http://webmineral.com/data/Nontronite.shtml

http://www.britannica.com/EBchecked/topic/120723/clay-mineral/80130/Mica-mineral-group

http://www.britannica.com/EBchecked/topic/120723/clay-mineral/80136/Imogolite-and-allophane#toc80137

Johnson, J.A., McDonald, R.G., Muir, D. and Tranne, J.-P., 2005. Pressure acid leaching of arid region nickel laterite ore: Part IV. Effect of acid loading and additives with nontronite ores. Hydrometallurgy 78, 264-270.

Kanungo, S.B., Das, R.P., 1988. Extraction of metals from manganese nodules of the Indian Ocean in aqueous solution of sulphur dioxide. Hydrometallurgy 20, 135-146.

Kanungo, S.B., Sukla, L.B. and Jena, P.K., 1988. Preferential extraction of cobalt from lateritic ore or concentrate by leaching in aqueous sulphur dioxide solution. Trans. Indian Inst. Metals 41, 527-533.

Kittelty, D.A., 2008. Low Eh leach with sulphur recycle, Int. Patent, WO2008/138038 A1, 20 Nov. 2008.

Komadel, P., Madejova, J., Stucki, J.W., 1995. Reduction and reoxidation of nontronite: questions of reversibility. Clays and Clay Minerals 43, 105-110.

Kumar, R., Das, S., Ray, R.K. and Biswas, A.K., 1993. Leaching of pure and cobalt bearing goethites in sulphurous acid: kinetics and mechanism. Hydrometallurgy 32, 39-59.

Kyle, J.H., 1996. Pressure acid leaching of Australian nickel/cobalt laterites. Nickel '96 Mineral to Market, Kalgoorlie, WA, 27–29 Nov. Australasian Institute of Mining and Metallurgy, Melbourne, pp. 245–249.

Leake, B.E., 1997. Nomenclature of amphiboles: report of the subcommittee on amphiboles of the international mineralogical association, commission on new minerals and mineral names. The Canadian Mineralogist 35, 219-246.

Lee, H.Y., Kim, S.G., Oh, J.K., 2005. Electrochemical leaching of nickel from low-grade laterites. Hydrometallurgy 77, 263−268.

Levenspiel, O., 1972. Chemical Reactions Engineering. Wiley, New York.

Liu, H., Gillaspie, J.D., Lewis, C.A., Neudorf, D., Barnett, S., 2004. Atmospheric leaching of laterites with iron precipitation as goethite. In: Imrie, W.P., Lane, D.M. (Eds.), International Laterite Nickel Symposium, TMS, Warrendale, pp. 347−367.

McDonald, R.G. and Whittington, B.I., 2008a. Atmospheric acid leaching of nickel laterites review. Part I. Sulphuric acid technologies. Hydrometallurgy 91, 35-55.

McDonald, R.G. and Whittington, B.I., 2008b. Atmospheric acid leaching of nickel laterites review. Part II. Chloride and bio-technologies. Hydrometallurgy 91, 56-69.

Newman, A.C.D. and Brown, G., 1987. The chemical constitution of clays. In: A.C.D. Newman (Ed.), Chemistry of Clays and Clay Minerals. Mineralogical Society Monographs, pp. 1-128.

Oelkers, E.H., 2001. General kinetic description of multioxide silicate mineral and glass dissolution. Geochimica et Cosmochimica Acta, 65(21): 3703-3719.

ÖNal, M., 2006. Determination of chemical formula a smectite. Commun. Fac. Sci. Univ. Ank. Series B 52(2), 1-6.

Papangelakis, V.G., Georgiou, D. and Rubisov, D.H., 1996. Control of iron during the sulphuric acid pressure leaching of limonitic laterites. In: Dutrizac, J.E. and Harris, G.B. (Eds.), Iron Control and Disposal. Canadian Institute of Mining, Metallurgy and Petroleum, Montreal, pp. 263-274.

Parhi, P. K., Park, K. H., Senanayake, G., 2013. A kinetic study on hydrochloric acid leaching of nickel from Ni-Al$_2$O$_3$ spent catalyst. Journal of Industrial and Engineering Chemistry 19, 589-594.

Petrie, M.L., 1995. Molecular interpretation for SO$_2$ dissolution kinetics of pyrolusite, magnetite and hematite. Applied Geochemistry 10, 253-267.

Rubisov, D.H., Krowinkel, J.M. and Papangelakis, V.G., 2000. Sulphuric acid pressure leaching of laterites − universal kinetics of nickel dissolution for limonites and limonitic/saprolitic blends. Hydrometallurgy 58, 1-11.

Rubisov, D.H., Papangelakis, V.G., 2000. Sulphuric acid pressure leaching of laterites ― speciation and prediction of metal solubilities at temperature. Hydrometallurgy 2000, 13-26.

Senanayake, G., 2011. Acid leaching of deep-sea manganese nodules − A critical review of fundamentals and applications. Minerals Engineering 24, 1379-1396.

Senanayake, G., Childs, J., Akerstrom, B.D., Pugaev, D., 2011. Reductive acid leaching of laterite and metal oxides ― A review with new data for Fe(Ni,Co)OOH and a limonitic ore. Hydrometallurgy 110, 13-32.

Senanayake, G., Das, G.K., 2004. A comparative study of leaching kinetics of limonitic laterite and synthetic iron oxides in sulphuric acid containing sulphur dioxide, Hydrometallurgy 72, 59-72.

Surana, V.S. and Warren, I.H., 1969. The leaching of goethite. Trans Inst. Min. Metall. Sec. C, C133-139.

Tindall, G. P. and Muir, D. M. (1996) Transformation of iron oxide in nickel laterite processing. Proc. Second. Inr. Symp. on Iron Conrrol 61 Hydromerallurgy, Iron Control and Disposal, Dutrizac, J. E. and Harris, G. B. Eds., CIM (Montreal), pp. 249-262.

Valenzuela-Diaz, F.R., Souza-Santos, P., 2001. Studies on the acid activation of Brazilian smectite clays. Quim.Nova 24, 345-353.

Warren, I.H. and Hay, M.G., 1974. Leaching of iron oxides with aqueous sulphur dioxide. Trans Inst. Min. Metall. Sec. C, C49-53.

Watling, H.R., Elliot, A.D., Fletcher, H.M., Robinson, D.J. and Sully, D.M., 2011. Ore mineralogy of nickel laterites: controls on processing characteristics under simulated heap-leach conditions. Australian Journal of Earth Sciences, 58: 725-744.

Whittington, B.I. and Johnson, 2005. Pressure acid leaching of arid region nickel laterite ore: Part III. Nickel losses in the residue. Hydrometallurgy 78, 256-263.

Whittington, B.I. and Muir, D., 2000. Pressure acid leaching of nickel laterites: a review. Min. Proc. Ext. Met. Rev. 21, 527-600.

Zhang, W., Singh, P., Muir, D.M., 2002. Oxidative precipitation of manganese with SO_2/O_2 and separation of cobalt and nickel. Hydrometallurgy 63, 127–135.

Figure Captions

Fig. 1. Schematic diagram of smectite crystal structure (Valenzuela-Diaz and Souza-Santos, 2001; http://agushoe.files.wordpress.com/2011/05/clay-structure.png).

Fig. 2. Elemental correlation in ores based on assays (from Table 2).

Fig. 3. XRD pattern of a) feed ore C, b) 10 h leach residue without Cu(II)/SO$_2$ and c) 10 h leach residue with Cu(II)/SO$_2$. (Non = Nontronite minerals, Ch = chlorite minerals, Amph = amphibole minerals, Kao = kaolinite, Goe = goethite, Q = quartz).

Fig. 4. Effect of lixiviants on leaching of metals from D (from Table 5).

Fig. 5. Comparison of leaching efficiencies (LE) of Ni (a), Fe (b), Co (c) and Mn (c) from smectite ores A, B, C and D in H$_2$SO$_4$ (dashed lines and open symbols) and H$_2$SO$_4$/Cu(II)/SO$_2$ (solid lines and closed symbols); Leach conditions: PD= 35% (w/w) for A,B and C, 20% (w/v) for D; acid = 700 kg/t ore for A, B, C, 600 kg/t for D; T = 90°C; SO$_2$ = 0.45 L/min; Cu(II) = 1 g/L; data for A,B and C from this work, D from Das and Lange (2011).

Fig. 6. Correlation between leaching efficiencies of nickel and iron during leaching of ores A, B, C and D in H$_2$SO$_4$ (open circles) and H$_2$SO$_4$/Cu(II)/SO$_2$ (closed circles) (data from Figs. 5a-d).

Fig. 7. Correlation between leaching efficiencies of nickel and iron during leaching of ores A, B, C and D in H$_2$SO$_4$ (open circles) and H$_2$SO$_4$/Cu(II)/SO$_2$ (closed circles) (data from Figs. 5a-d).

Fig. 8. Effect of composition of Fe element or Fe minerals in ores A, B, C and D on correlation slopes of LE$_{(Ni)}$ and LE$_{(Fe)}$ during reductive leaching with H$_2$SO$_4$/Cu(II)/SO$_2$ (Fe element/mineral compositions from Tables 2 and 3, slopes from Figs. 7(a) to (d)).

Fig. 9. Effect of molar ratio of Fe/(Fe+Mg+Si) in ores A, B, C and D on correlation slopes and intercepts and LE$_{(Ni)}$ during non-reductive leaching in H$_2$SO$_4$ (AAL) and reductive leaching in H$_2$SO$_4$/Cu(II)/SO$_2$ (RAAL) after 0.5 h (molar ratio from Table 2, intercepts and slopes from Figs. 7(a) to (d), LE$_{(Ni)}$ from Table 7).

Fig. 10. Correlation between leaching efficiencies of Mn, Co, Ni and Fe during leaching of ore C in H$_2$SO$_4$ (open circles and dashed lines-AAL) and H$_2$SO$_4$/Cu(II)/SO$_2$ (closed circles and solid lines-RAAL) (data from Figs. 5a-d).

Fig.11. Arrhenius plot for initial leaching of nickel from ore-D in first 0.5 h (data from Das and Lange, 2011).

Fig. 12. Applicability of shrinking core model for leaching metals from ore A in H$_2$SO$_4$ (see Figs. 5a-d for other conditions).

Fig.13. Relationship between apparent rate constant (k_{ap}) and initial rates (dX/dt) for metal leaching from ores A-D under non-reducing (AAL) or reducing (RAAL) conditions (dX/dt based on 0.5 h data from Table 7, k_{ap} from Table 8).

Fig. 14. Log-log plot of initial fraction of metal leached from ore D in first 0.5 h as a function of initial acid concentration (data from Table 8).

Fig. 15. Logarithmic correlation of apparent rate constant for nickel leaching from manganese nodules and laterite ores (limonite and smectite) and H^+ concentration. Data from Tables 6 and 8 (smectite ores A-D) and Senanayake, 2011 (nodules and limonitic laterite ore).
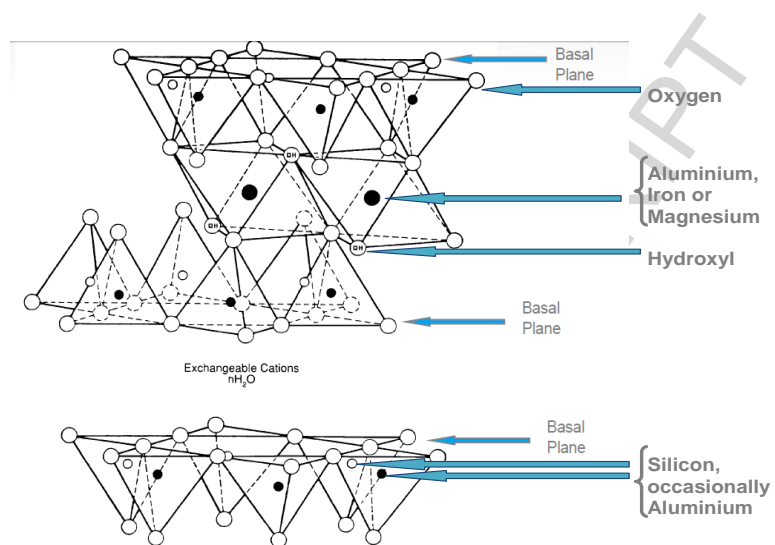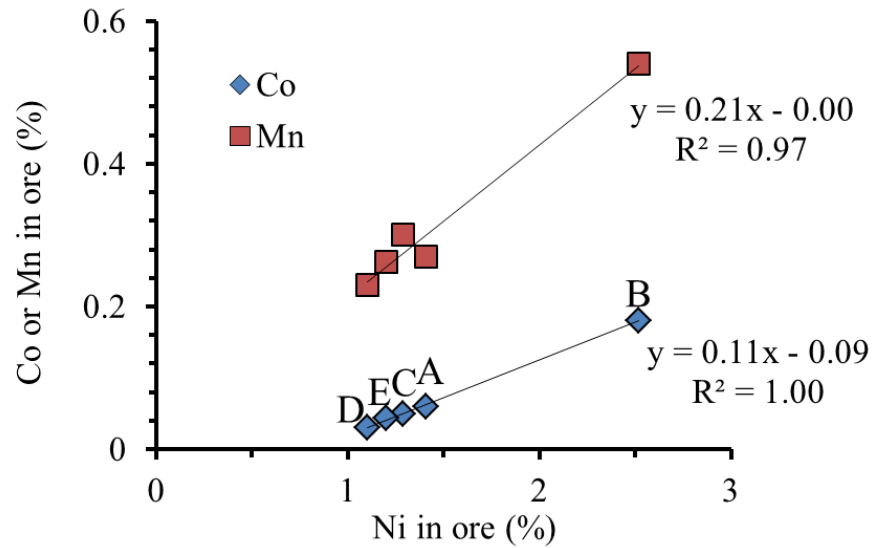
Figure 1

Fig. 1. Schematic diagram of smectite crystal structure (Valenzuela-Diaz and Souza-Santos, 2001; http://agushoe.files.wordpress.com/2011/05/clay-structure.png)
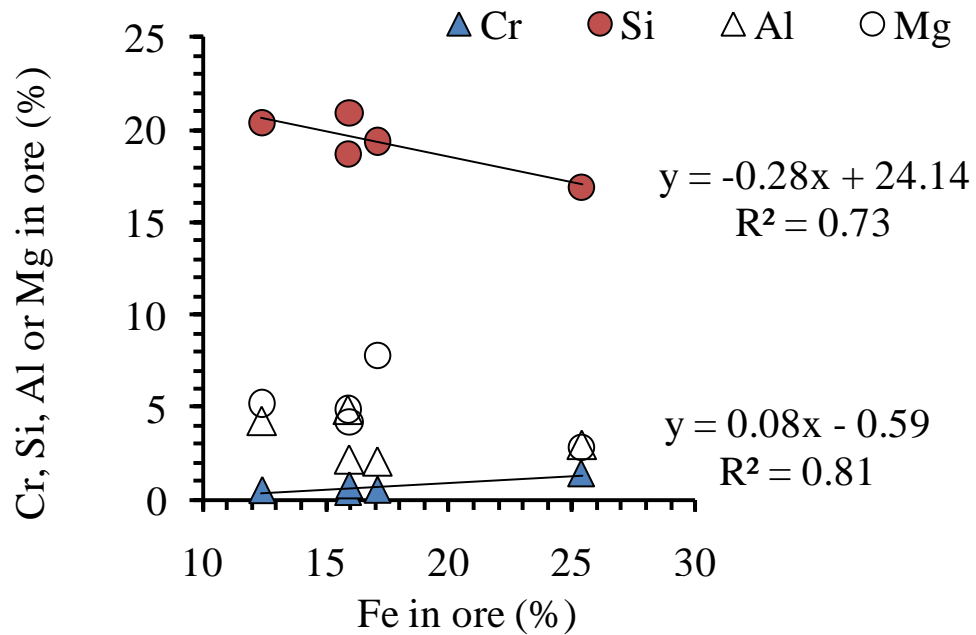
Figure 2

(a)

(b)

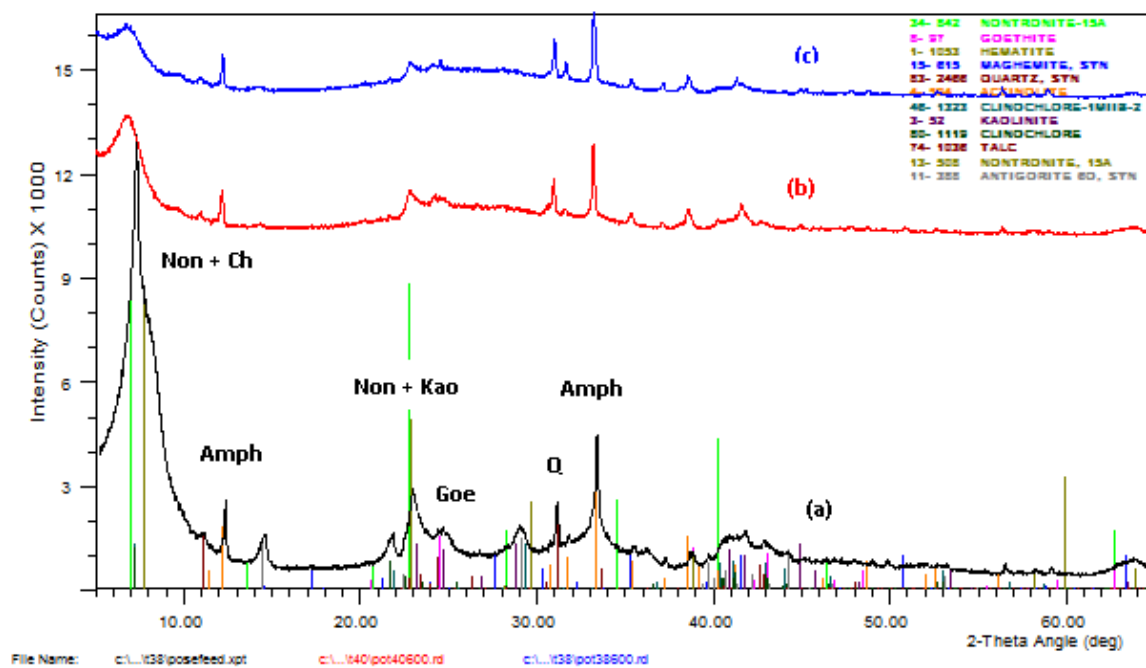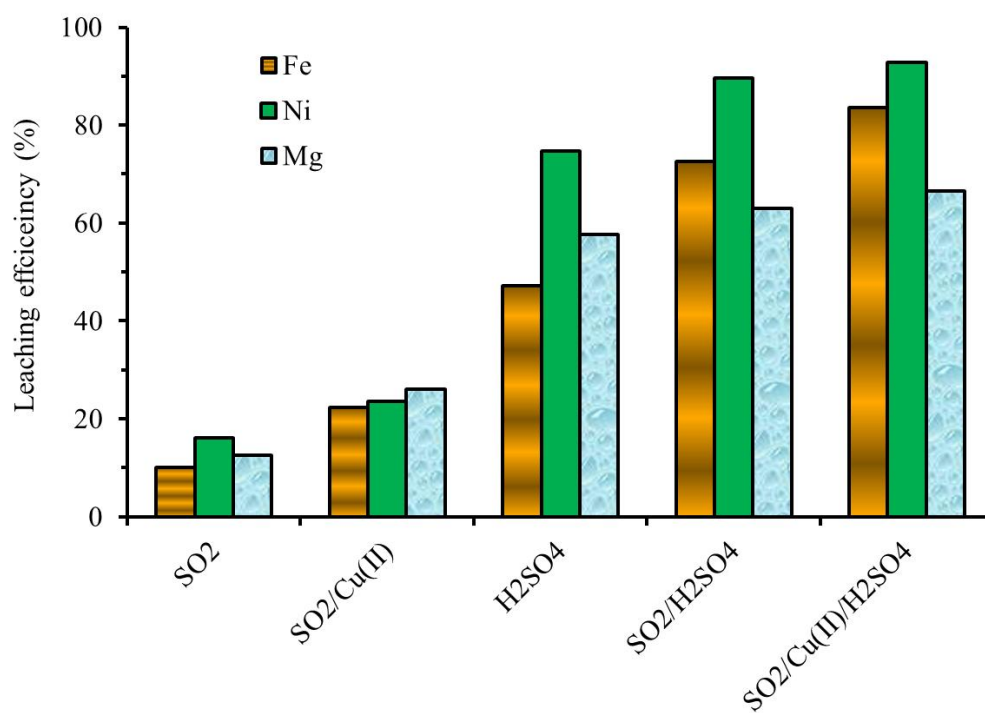Fig. 2. Elemental correlation in ores based on assays (from Table 2)

Figure 3

Fig. 3. XRD pattern of a) feed ore C, b) 10 h leach residue without Cu(II)/SO$_2$ and c) 10 h leach residue with Cu(II)/SO$_2$. (Non = Nontronite minerals, Ch = chlorite minerals, Amph = amphibole minerals, Kao = kaolinite, Goe = goethite, Q = quartz)
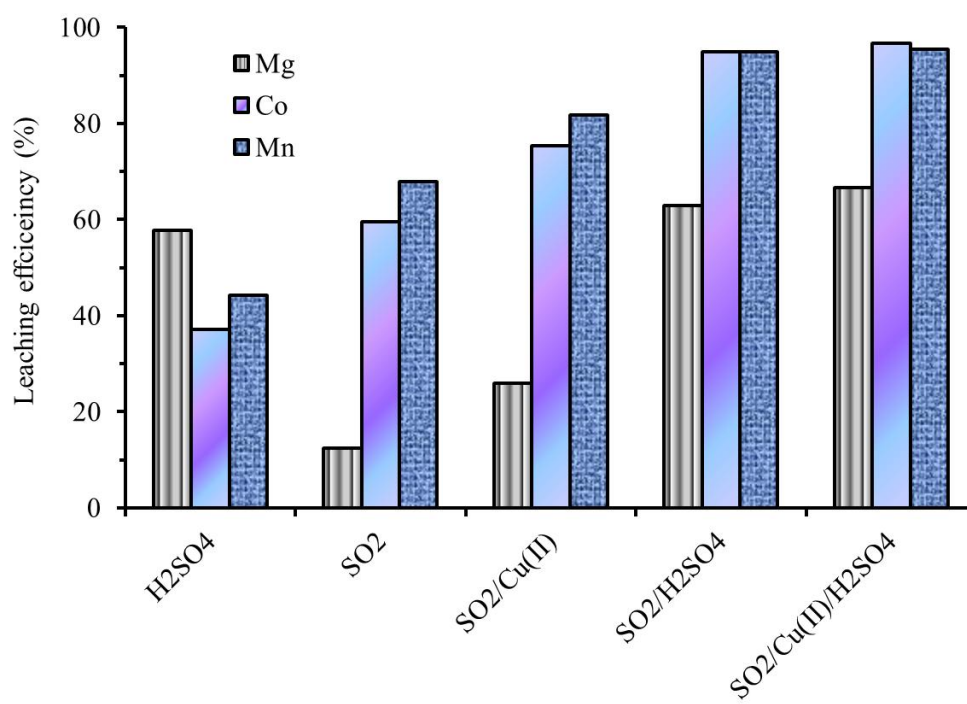
Figure 4
(a)

(b)

Fig.4. Effect of lixiviants on leaching of metals from ore D (from Table 5)
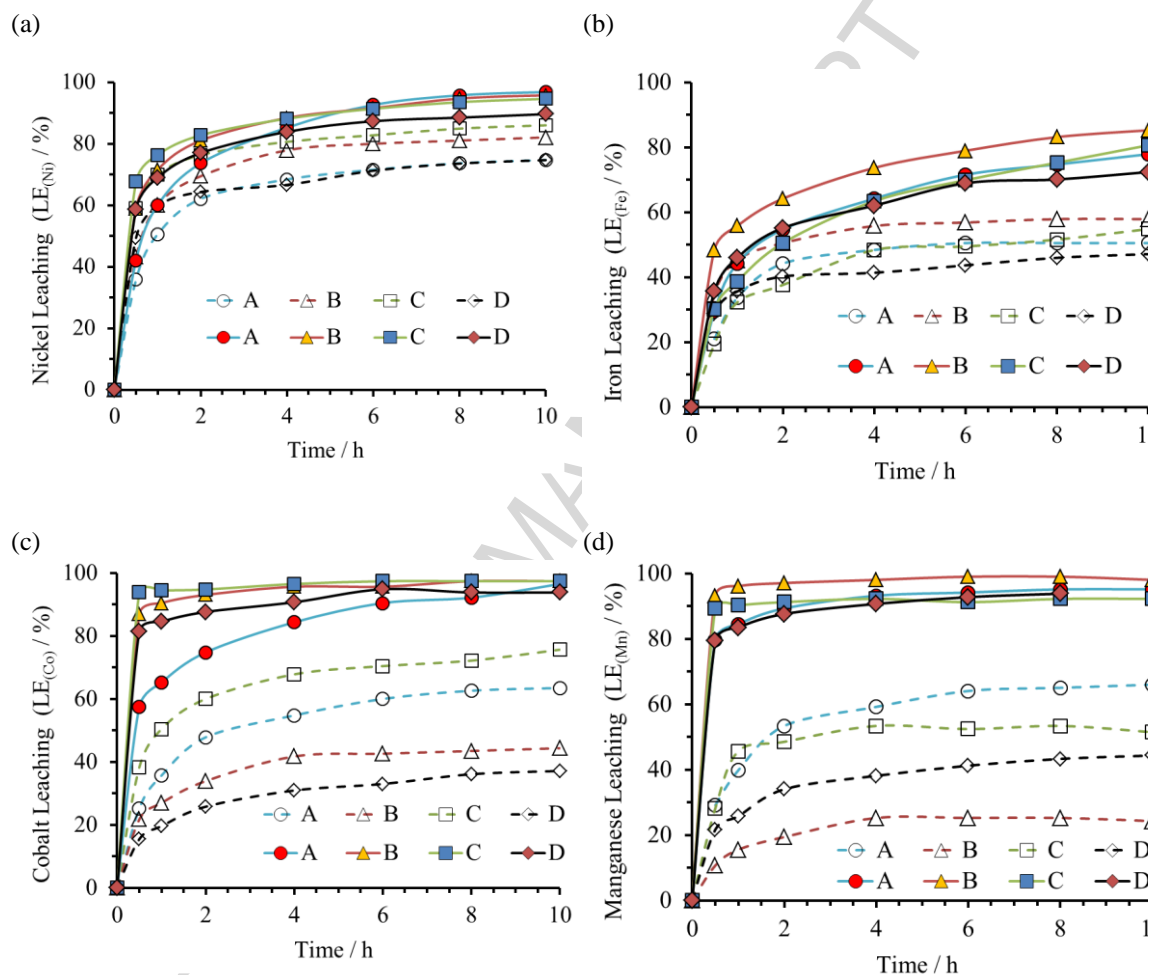
Figure 5

(a)

(b)

(c)

(d)

Fig. 5. Comparison of leaching efficiencies (LE) of Ni (a), Fe (b), Co (c) and Mn (c) from smectite ores A, B, C and D in H_2SO_4 (dashed lines and open symbols) and $H_2SO_4/Cu(II)/SO_2$ (solid lines and closed symbols); Leach conditions: PD= 35% (w/w) for A,B and C, 20% (w/v) for D; acid = 700 kg/t ore for A, B, C, 600 kg/t for D; T = 90°C; SO_2 = 0.45 L/min; Cu(II) = 1 g/L; data for A,B and C from this work, D from Das and Lange (2011).

Figure 6

Fig.6. Correlation between leaching efficiencies of nickel and iron during leaching of ores A, B, C and D in H_2SO_4 (open circles) and $H_2SO_4/Cu(II)/SO_2$ (closed circles) (data from Figs. 5a-d).
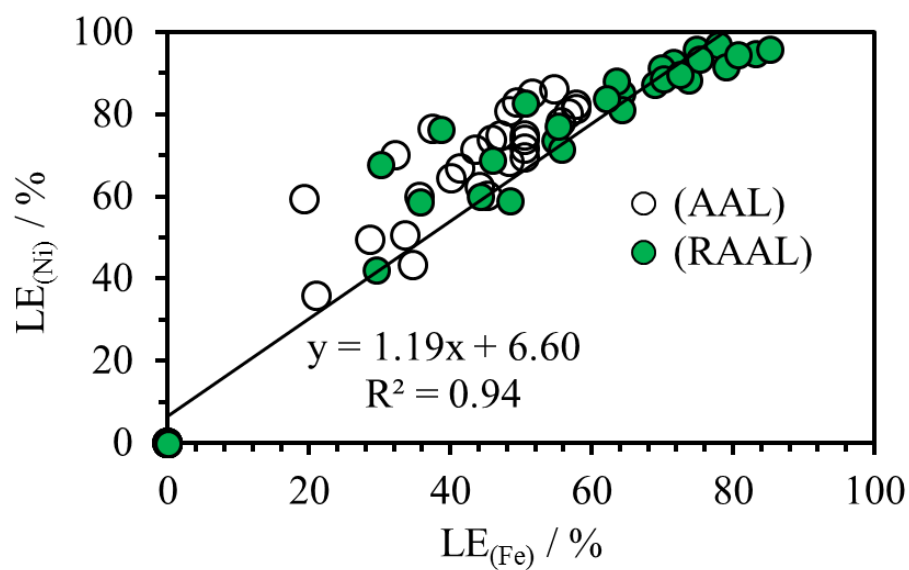
Figure 7

(a)

(b)

(c)

(d)

Fig.7. Correlation between leaching efficiencies of nickel and iron during leaching of ores A, B, C and D in H_2SO_4 (open circles) and $H_2SO_4/Cu(II)/SO_2$ (closed circles) (data from Figs. 5a-d).

Figure 8

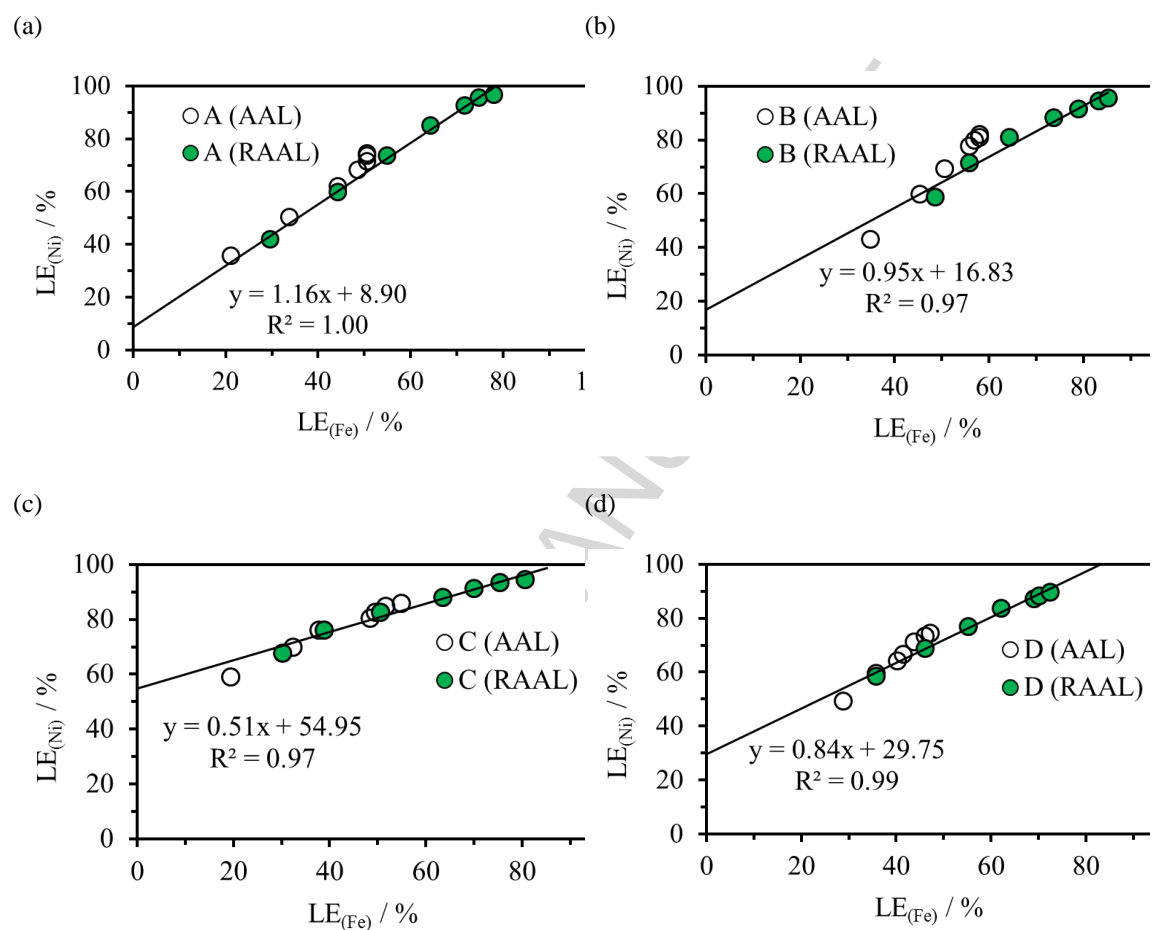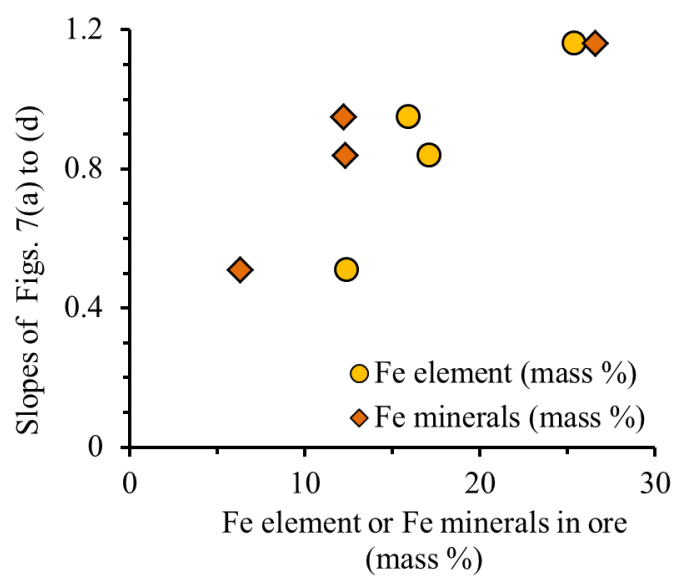Fig. 8. Effect of composition of Fe element or Fe minerals in ores A, B, C and D on correlation slopes of $LE_{(Ni)}$ and $LE_{(Fe)}$ during reductive leaching with $H_2SO_4/Cu(II)/SO_2$ (Fe element/mineral compositions from Tables 2 and 3, slopes from Figs. 7(a) to (d)).

Figure 9
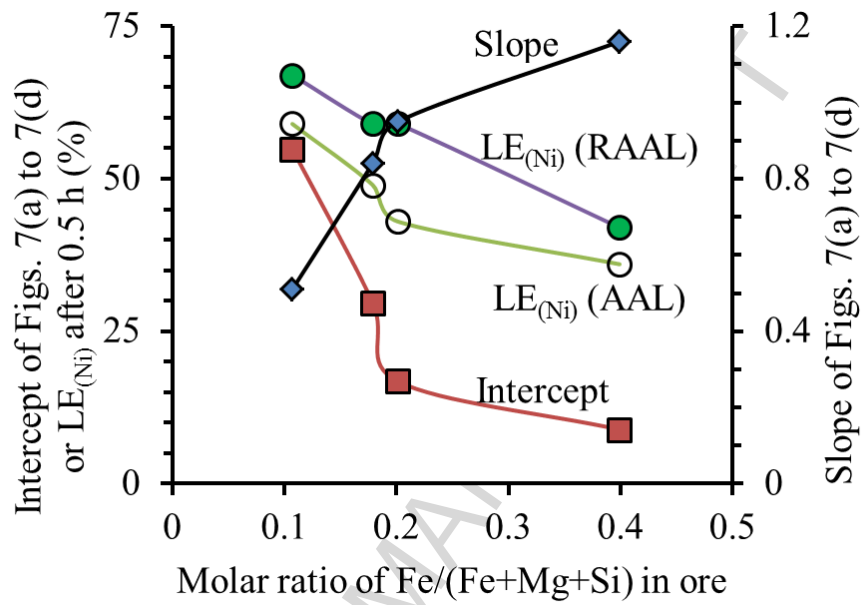
Fig. 9. Effect of molar ratio of Fe/(Fe+Mg+Si) in ores A, B, C and D on correlation slopes and intercepts and $LE_{(Ni)}$ during non-reductive leaching in H_2SO_4 (AAL) and reductive leaching in $H_2SO_4/Cu(II)/SO_2$ (RAAL) after 0.5 h (molar ratio from Table 2, intercepts and slopes from Figs. 7(a) to (d), $LE_{(Ni)}$ from Table 7).

Figure 10
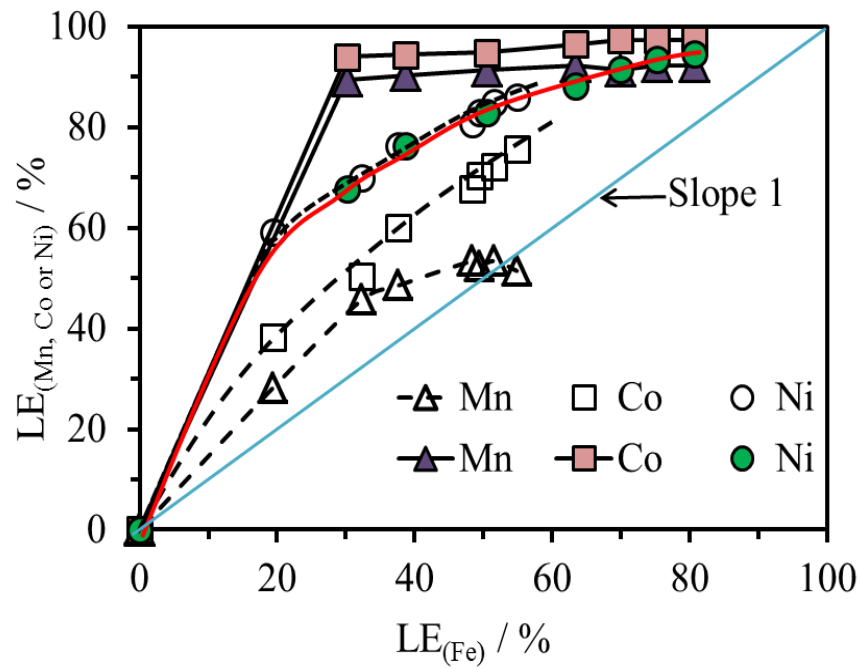
Fig. 10. Correlation between leaching efficiencies of Mn, Co, Ni and Fe during leaching of ore C in H_2SO_4 (open circles and dashed lines-AAL) and H_2SO_4/Cu(II)/SO_2 (closed circles and solid lines-RAAL) (data from Figs. 5a-d).

Figure 11
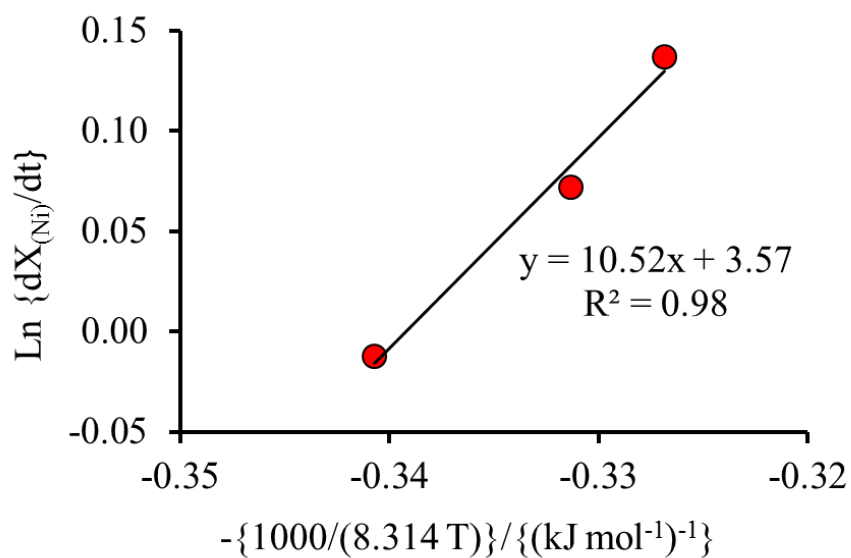
Fig.11. Arrhenius plot for initial leaching of nickel from ore D in first 0.5 h (data from Das and Lange, 2011)

Figure 12
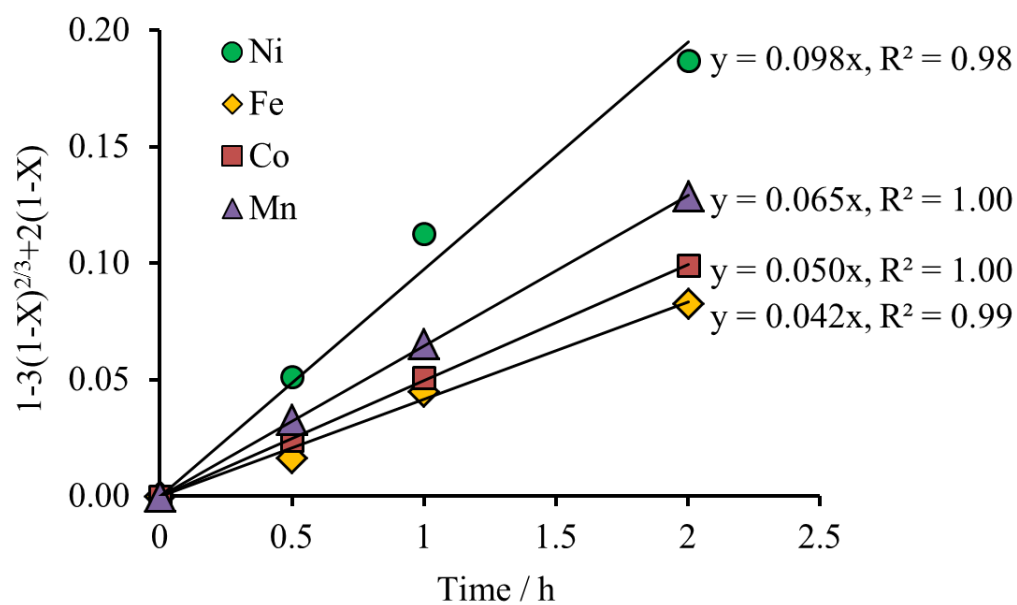
Fig. 12. Applicability of shrinking core model for leaching metals from ore A in H_2SO_4 (see Figs. 5a-d for other conditions).

Figure 13

(a)
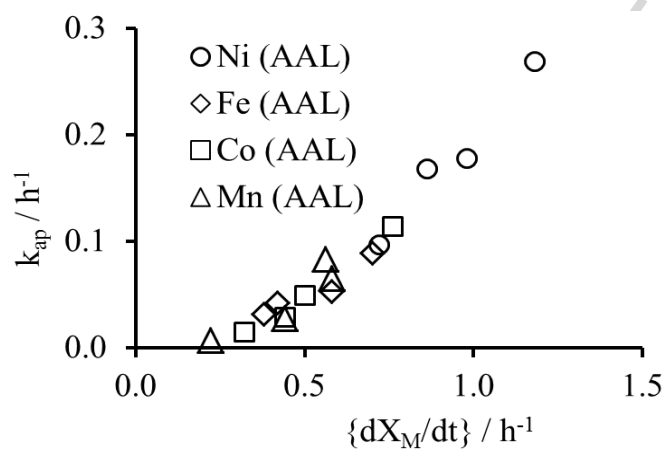
(b)
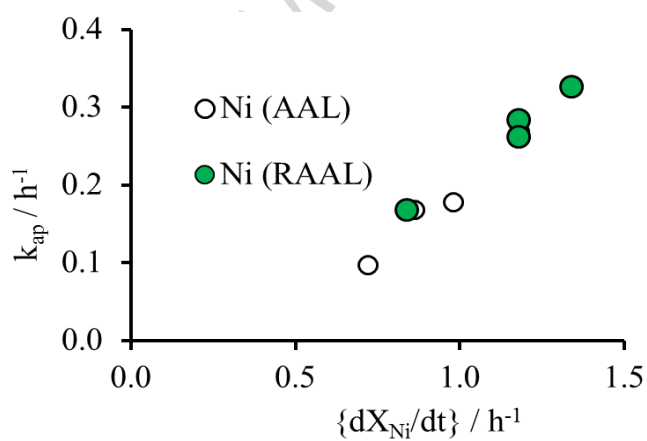
(c)
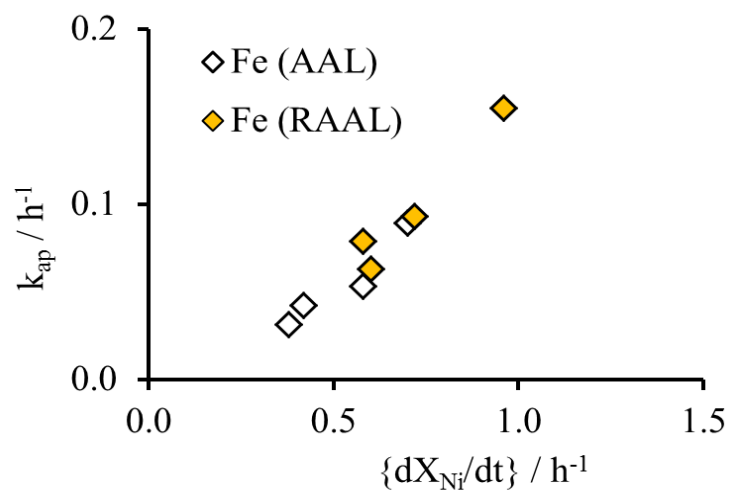
Fig.13. Relationship between apparent rate constant (k_{ap}) and initial rates (dX/dt) for metal leaching from ores A-D under non-reducing (AAL) or reducing (RAAL) conditions (dX/dt based on 0.5 h data from Table 7, k_{ap} from Table 8).

Figure 14

(a)
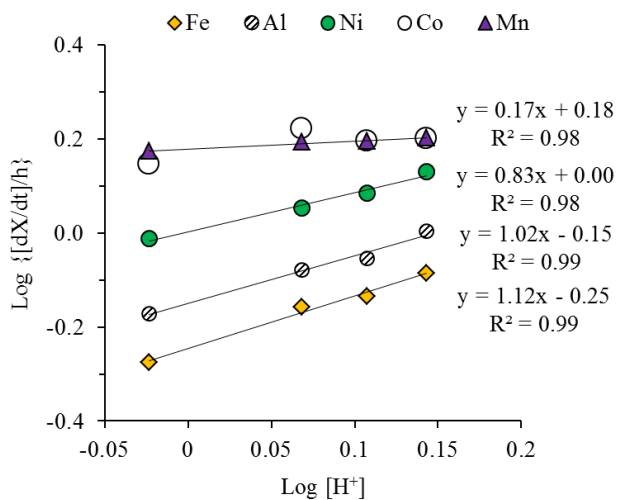
(b)
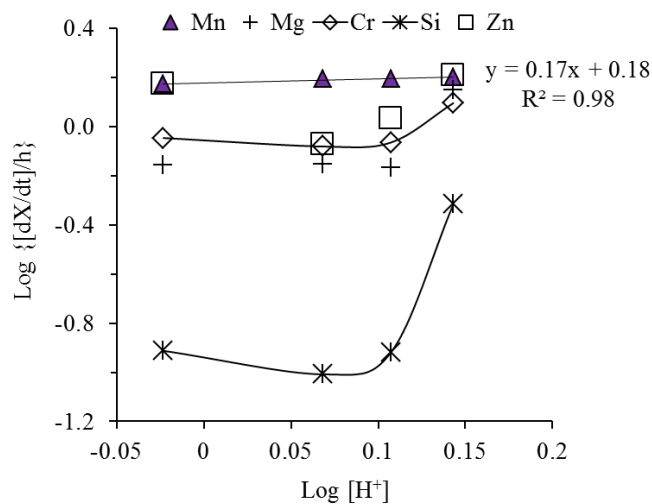
Fig. 14. Log-log plot of initial fraction of metal leached from ore D in first 0.5 h as a function of initial acid concentration (data from Table 8)

Figure 15
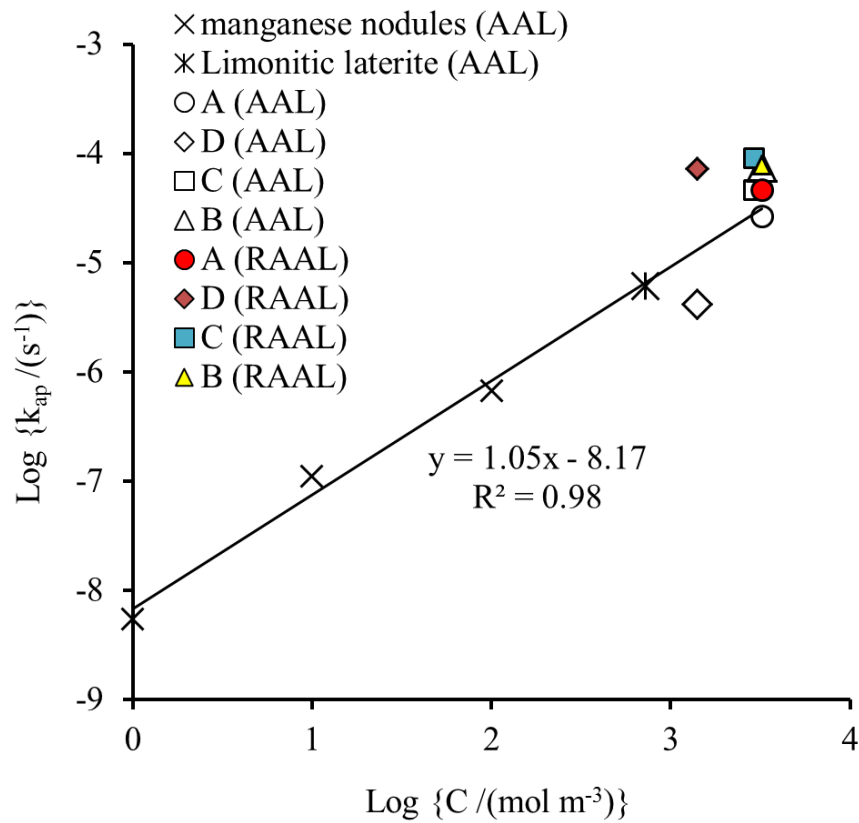
Fig. 15. Logarithmic correlation of apparent rate constant for nickel leaching from manganese nodules and laterite ores (limonite and smectite) and H^+ concentration. Data from Tables 6 and 8 (smectite ores A-D) and Senanayake, 2011 (nodules and limonitic laterite ore).

Table 1 Composition of oxides in some co-minerals in smectite ores

Oxide	Composition of oxide in mineral (mass %)			
	Nontronite[a]	Lizardite[b]	Amphibole[c]	Sodium montmorillonite[d]
SiO_2	36.4	30.4	51.6	61.6
Al_2O_3	10.3	21.2	7.39	21.1
MgO	-	33.9	18.1	1.98
Fe_2O_3	32.2	1.99	-	4.88
FeO	-	1.55	7.55	-
Na_2O	1.87	-	0.61	2.14
MnO	-	-	0.17	-
CaO	-	-	12.3	0.36
H_2O	18.2	12.1	-	6.90
K_2O	-	-	-	0.34
TiO_2	-	-	-	0.3

a. $M^+_{0.33}Fe^{3+}_2(Si_{3.67}Al_{0.33})O_{10}(OH)_2.nH_2O$
   (http://webmineral.com/data/Nontronite.shtml; Onal, 2006)
b. Brigatti et al., 1997
c. Leake, 1997
d. $M^+_{0.33}(Al_{1.67}Mg_{0.33})Si_4O_{10}(OH)_2.nH_2O$ (Onal, 2006)

Table 2. Chemical analysis of smectite ores

Smectite ore[a]	A	B	C	D[b]	E[c]
Ni	1.41	2.52	1.29	1.1	1.20
Co	0.06	0.18	0.05	0.03	0.04
Mn	0.27	0.54	0.30	0.23	0.26
Cr	1.40	0.40	0.50	0.52	0.76
Al	3.00	4.90	4.30	2.10	2.20
Mg	2.80	4.90	5.20	7.80	4.20
Fe	25.4	15.9	12.4	17.1	15.9
Si	16.9	18.7	20.4	19.4	20.9
As	-	-	-	-	0.02

a. This work unless stated otherwise, b. Das and Lange (2011), c. Buyukakinci and Topkaya (2009)

Table 3. Mineralogical components of different nickel lateritic ores

Mineral phase	Formula	Composition (%)				
		A	B	C	D[a]	E[b]
Smectite	$Mg_{0.2}(Fe_{1.2}Mg_{0.5}Ni_{0.1}Al_{0.3})(Si_{3.8}Al_{0.2})O_{10}(OH)_2.2H_2O$	-	-	-	59.9	p
Nontronite	$Na_{0.3}Ca_{0.1}Mg_{0.4}(Fe_{3.5}Ni_{0.3}Mg_{0.2})(Si_{7.3}Al_{0.6}O_{20}(OH)_4$[c]	57.9	66.3	66.7	-	-
Serpentine[d]	$\boldsymbol{X_{2\text{-}3}Si_2O_5(OH)_4}$ where $\boldsymbol{X}$ = Mg, Fe^{2+}, Fe^{3+}, Ni , Al, Zn, or Mn	0.8	0.2	0.3	11.3	-
Goethite	α-FeOOH	7.7	11.2	2.6	-	p
Hematite	α-Fe_2O_3	8.4	-	1.7	5.5	p
Maghemite/magnetite	γ-Fe_2O_3/Fe_3O_4	10.5	1.0	2.0	6.8	-
Chlorite	$(Mg,Fe(II),Mn,Ni)_{6-x-y}(Al,Fe(III),Cr)_y] [(Si_{4-z}Al_zO_{10}(OH)_8$[e]	0.9	3.4	1.7	2.0	-
Kaolinite	$Al_4Si_4O_{10}(OH)_8$	4.2	4.0	7.2	-	-
Quartz	SiO_2	1.1	0.4	4.0	-	p
Amphibole	$(Mg,Fe,Ca,Na)_{2-3}(Mg,Fe,Al)_5(Si,Al)_8O_{22}(OH)_2$	-	-	6.3	-	-
gypsum	$CaSO_4.2H_2O$	-	-	-	-	p
Unaccounted		8.5	13.0	7.0	13.8	-
Total		100	99.5	99.5	99.3	-

a. Data for ore D from Das and Lange (2011);

b. "p" indicates that these minerals are present in ore E (Buyukakinci and Topkaya, 2009);

c. Data from Tindall and Muir (1996)

d.   http://www.minerals.net/mineral/serpentine.aspx

e. Data from Bayliss (1975).

Table 4. Nickel grades in different laterite ores and leach residues

Solid	Leaching agent	H_2SO_4 (kg/t ore)	Pulp density (%)	Nickel grade (%)			
				A	B	C	D
Feed	Unleached feed	-	-	1.41	2.52	1.29	1.10
Residue	H_2SO_4	700	35	0.56	0.68	0.27	-
Residue	$H_2SO_4/Cu(II)/SO_2$	700	35	0.09	0.23	0.12	-
Residue	$H_2SO_4/Cu(II)/SO_2$	600	35	-	-	-	0.07
			30	-	-	-	0.09
			25	-	-	-	0.11
			20	-	-	-	0.14

Note: Leach duration 10 h at 90°C

Table 5 Leaching efficiencies of metals from ore D

SO$_2$ (L/min)	Cu(II) (g/L)	Test	Lixivient	Leaching efficiency (LE/%)				
				Fe	Ni	Co	Mn	Mg
0	0	i)	H$_2$SO$_4$	47.1	74.7	37.1	44.3	57.7
0.45	0	ii)	SO$_2$	10.3	16.1	59.8	67.0	12.5
0.45	1	iii)	SO$_2$/Cu(II)	22.4	23.6	75.4	81.7	26.0
0.45	0	iv)	SO$_2$/H$_2$SO$_4$	72.5	89.7	95.0	95.0	63.0
0.45	1	v)	SO$_2$/Cu(II)/H$_2$SO$_4$	83.6	92.8	96.7	95.5	66.6

Other conditions: p.d. 20% (w/w), temp. 90°C, H$_2$SO$_4$ 600 kg/t ore (where added).

Table 6. Effect of acid dosage on nickel leaching efficiencies from different smectite ores

Ore	Pulp density (w/w %)	Temp(°C)	Reductants for RAAL		Acid (kg/t ore)	Initial acid concn. (g/L)	Final liquor acid concn. (g/L)		Leach time (h)	LE$_{(Ni)}$ (%)	
			SO$_2$ flowrate (L/min)	Cu (II) (kg//t ore)[a]			AAL	RAAL		AAL	RAAL
A	35	90	0.45	1.8	600	278	-	51.8	10	-	93.2
		90	0.45	1.8	700	315	31.6	67.2	10	75.1	96.9
B	35	90	0.45	1.8	700	316	26.6	46.7	10	82.2	95.1
C	35	90	0.45	1.8	600	324	-	32.6	10	-	89.1
		90	0.45	1.8	700	287	43.4	64.1	10	85.8	94.4
D	20	90	0.45	4.0	400	92.9	-	20.1	6	-	73.6
		90	0.45	4.0	500	115	-	25.8	6	-	84.0
		90	0.45	4.0	600	136	30.9	20.6	6	71.3	91.5
		90	0.45	4.0	600	136	-	11.1	10	-	93.4
		90	0.45	-	600	136	28.5	36.0	10	74.7	90.5
		80	0.45	-	600	136	-	39.4	10	-	85.7
		95	0.45	-	600	136	-	-	10	-	91.4
	35	90	0.45	1.8	600	136	11.0	29.2	10	82.8	96.5
E	20[b]	95	-	-	-	98	-	-	5	62.7	-
		95	-	-	-	196	-	-	5	91.1	-
		95	-	-	-	245	-	-	5	96.1	-
		95	-	-	-	98	-	-	24	65.4	-
		95	-	-	-	196	58.2	-	24	96.0	-
		95	-	-	960	245	-	-	24	98.6	-

a. Cu(II) addition in this table is reported based on kg/t of ore which corresponds to ~1 g/L Cu(II) in soln.

b. w/v%

Table 7. Summary of leaching efficiency of metals under non-reducing and reducing conditions

Ore / Metal	Time / h	Leaching efficiency (LE / %)							
		A		B		C		D	
		AAL	RAAL	AAL	RAAL	AAL	RAAL	AAL	RAAL
Ni	0.5	36	42	43	59	59	67	65	59
	6	72	93	80	92	83	91	82	87
	10	75	97	82	95	86	94	83	97
Fe	0.5	21	29	35	48	19	30	29	40
	6	50	72	57	79	49	70	44	69
	10	51	78	58	85	55	81	47	79
Co	0.5	25	57	22	87	38	94	34	87
	6	60	90	43	96	70	97	59	95
	10	64	97	44	97	76	97	63	97
Mn	0.5	29	80	11	93	28	89	27	87
	6	64	94	25	99	52	91	51	96
	10	66	95	24	98	51	92	53	96
Mg	10	91	94	88	93	78	82	78	87

Test conditions: p.d. 35% w/w, temp. 90 °C, H_2SO_4 700kg/t ore for ores A, B and C, H_2SO_4 600 kg/t ore for ore D, SO_2 flow rate 0.45 L/min (only for RAAL), Cu(II) ~1 g/L (only for RAAL).

Table 8. Apparent rate constant of shrinking core model for leaching metals from ores A-D

Ore / metal	Apparent rate constant (k_{ap}/h^{-1})							
	A		B		C		D	
	AAL	RAAL	AAL	RAAL	AAL	RAAL	AAL	RAAL
Ni	0.097	0.167	0.168	0.283	0.269	0.326	0.178	0.261
Fe	0.042	0.079	0.089	0.155	0.031	0.063	0.053	0.093
Co	0.049	-	0.029	-	0.114	-	0.015	-
Mn	0.065	-	0.007	-	0.083	-	0.027	-

See Figs. 5a-d for other conditions

Table 9. Effect of initial acid concentration on metal leaching efficiency of ore D under non-reducing conditions

Acid dosage (kg/t)	H₂SO₄ (mol/L)		Leaching efficiency of metals from ore D after 0.5 h (LE / %)								
	t = 0 h	t = 0.5 h	Al	Fe	Ni	Co	Mn	Mg	Zn	Cr	Si
400	0.95	0.48	33.7	26.5	48.6	70.1	74.5	34.8	74.7	44.9	6.1
500	1.17	0.63	41.7	34.8	56.4	83.4	77.9	35.0	42.4	41.5	4.9
550	1.28	0.69	44.2	36.6	60.8	78.2	78.5	34.1	53.8	43.0	6.0
600	1.39	-	50.4	41.1	67.4	79.5	79.5	70.3	80.8	62.3	24.1

Test conditions: p.d. 20% w/w, temp. 90 °C, SO₂ flowrate 0.45 L/min, H₂SO₄ 600 kg/t ore

Highlights:

- Reductive atmospheric acid leaching of lateritic different smectite ores in $H_2SO_4/Cu(II)/SO_2$ is compared.
- The extractions of Ni, Co, Mn and Fe from the different ores were 90-97%, 94-97%, 92-98% and 72-85% respectively.
- The initial leaching of Ni, Co, Mn and Fe from smectite ores obeys shrinking core kinetics.
- The logarithmic correlation of apparent rate constant for Ni leaching and H^+ concentration follow the same linear relationship as that reported for manganese nodules and limonitic laterite.